AJNR

Sensitivity-Encoded Diffusion Tensor MR Imaging of the Cervical Cord

Mara Cercignani, Mark A. Horsfield, Federica Agosta and Massimo Filippi

AJNR Am J Neuroradiol 2003, 24 (6) 1254-1256
http://www.ajnr.org/content/24/6/1254

AJNR Am J Neuroradiol 24:1254–1256, June/July 2003

Technical Note

Sensitivity-Encoded Diffusion Tensor MR Imaging of the Cervical Cord

Mara Cercignani, Mark A. Horsfield, Federica Agosta, and Massimo Filippi

Summary: The aim of this study was to apply sensitivity-encoding (SENSE) echo-planar imaging (EPI) to diffusion tensor MR imaging of the cervical cord, an anatomic region where MR imaging is particularly challenging. This technique was implemented with a SENSE reduction factor of 2 and used for imaging a water phantom and five healthy volunteers. Off-resonance artifacts were notably reduced compared with those of full-FOV EPI sequences. This approach to diffusion tensor MR imaging of the cervical cord is promising for future, more extensive clinical applications.

The highly ordered arrangement of axons in the spinal cord makes diffusion measurements particularly interesting in this anatomic structure. However, image distortion caused by susceptibility variation, together with the artifacts caused by surrounding lipid and partial voluming from CSF, prevent the use of single-shot echo-planar imaging (EPI) in the cord. This work describes the implementation of a sensitivity-encoded (SENSE) (1) single-shot EPI pulse sequence for diffusion tensor (DT) (2) MR imaging of the cervical cord. In SENSE imaging, the duration of the echo train is reduced by a faster filling of the k space, resulting in a wider bandwidth in the phase-encoded direction and, therefore, reduced image distortion (1, 3). SENSE EPI sequences for DT MR imaging have been successfully applied in the brain (4, 5). In this study, the sequence was used to collect data from a water phantom and from a group of healthy volunteers, with the aim of measuring the DT and assessing the feasibility of using the technique in the cervical cord, as a preliminary step toward its clinical use.

Description of the Technique

All imaging was performed by using a 1.5-T scanner (Magnetom Vision; Siemens, Erlangen, Germany) with a maximum gradient strength of 21 mT/m and a maximum slew rate of 167 T/m/s. The same imaging protocol was performed with a water phantom and in five healthy volunteers (three women and two men; mean age [SD], 26.4 years [3.9]). One subject was imaged twice after a 7-day interval. The protocol consisted of a 2D gradient-echo (GE) sequence (TR/TE, 900/15; flip angle; 70°; matrix, 64 × 64; FOV, 240 × 240 mm; number of sections, five; sagittal plane; section thickness, 4 mm). This sequence was repeated twice: once by using the manufacturer's four-element phased-array neck coil and once by using the body coil for signal intensity reception. The protocol also included a SENSE single-shot EPI (reduction factor, $R = 2$; 7000/100; FOV, 240 × 90 mm; matrix, 128 × 48; echo train, ≈ 40 ms; number of sections, five; sagittal plane; section thickness, 4 mm). This sequence collected 16 images per section, including two images with no diffusion weighting ($b \approx 0$ s/mm^2) and 14 images with the same b factor of 900 s/mm^2 but with gradients applied in different directions. The diffusion unweighted images were needed to compute the DT, and the gradient orientations were chosen according to the algorithm proposed by Jones et al (6), which was designed to optimize DT MR imaging acquisition. The measurement was repeated four times to improve the signal-to-noise ratio (SNR). Three saturation bands were used, positioned in the anterior part of the neck and transversely at the edges of the FOV in the vertical direction. The phase-encoded direction was anteroposterior, and total imaging time was about 10 minutes. The water phantom was also scanned by using a standard full-FOV (240 × 240 mm) diffusion-weighted EPI sequence, with parameters otherwise identical to those of the SENSE sequence.

Sensitivity-encoded data were reconstructed offline as described by Pruessman et al (1). Spatially varying matrix regularization (4, 7, 8) was also used to increase the tolerance to error, as the inverse solution can be ill conditioned. There are several ways for the assessment of the spatial sensitivity of the coils (1, 4, 9). We divided each of the (complex) single-coil GE images by the corresponding body coil GE image. The resulting images were then smoothed by fitting a third-order polynomial (1). Once unwrapped, the diffusion-weighted images were magnitude averaged to improve the SNR.

Despite the reduction of the number of k-space lines, geometric distortion due to eddy currents was still present. In the SENSE reconstruction algorithm, all voxels that lie outside the imaged object in the body-coil image are excluded, as they contribute no signal intensity (1). As a consequence, retrospective estimation and correction of the eddy current induced geometrical distortion, such as that proposed by Haselgrove and Moore (10), is not directly applicable to SENSE images. The distortion was measured on the images collected from a phantom filled with silicon oil, by using a full-FOV single-shot EPI sequence (matrix, 128 × 128; FOV, 240 × 240 mm) but with parameters otherwise identical to those of the SENSE sequence. Silicon oil was chosen because of its low diffusion coefficient, which results in similar image contrast for the unweighted and diffusion-weighted images (11). A reference image was calculated as the average of the two non–diffusion-weighted images available for each section, and then a registration algorithm based on maximizing the mutual information (12) between the reference image and the corrected image was

Received November 18, 2002; accepted after revision, January 29, 2003.

From the Neuroimaging Research Unit, Department of Neuroscience, Scientific Institute and University Ospedale San Raffaele, Milan, Italy (M.C., F.A., M.F.); and the Division of Medical Physics, University of Leicester, Leicester Royal Infirmary, United Kingdom (M.A.H.).

This study was supported by a grant from the Fondazione Italiana Sclerosi Multipla (FISM 2000/R/37).

Address reprint requests to Massimo Filippi, Neuroimaging Research Unit, Department of Neuroscience, Scientific Institute and University Ospedale San Raffaele, via Olgettina 60, 20132 Milano, Italy.

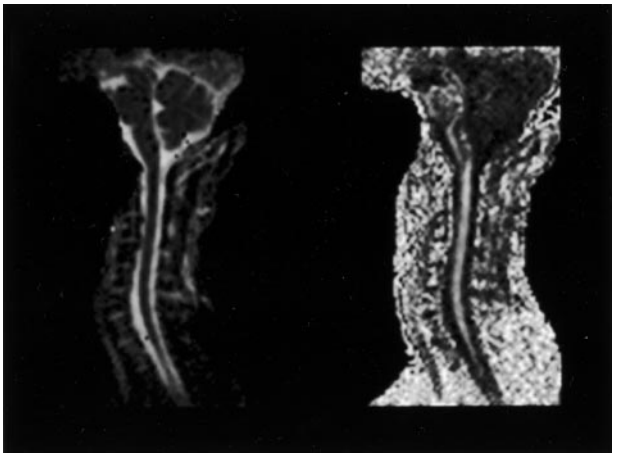

FIG 1. Mean diffusivity (*left*) and FA (*right*) maps obtained in a healthy volunteer by using the SENSE EPI sequence. The advantage of SENSE over standard EPI is the reduction of off-resonance artifacts due to an increased bandwidth in the phase-encoding direction. As a consequence, images are less sensitive to susceptibility variations. The aliasing caused by the reduction of the FOV can be resolved by exploiting the coil sensitivity as a signal intensity encoding. In this study, the standard four-element neck coil was used to show the feasibility of the technique on a commercial machine with no dedicated hardware.

applied. The distortion for each diffusion-weighted image collected by using the SENSE sequence was estimated by scaling the measured distortion by a factor equal to the ratio of the number of k-space lines for the two sequences. The DT was calculated for each voxel by using linear regression (2), and the eigenvalues and eigenvectors of the tensor matrix were derived after matrix diagonalization. The eigenvalues were averaged to give the mean diffusivity ($\bar{D}$) and used to calculate the fractional anisotropy (FA) (13).

Phantom data collected by using the full-FOV sequence underwent a direct correction for eddy currents and then the same DT calculation as that described for the SENSE data.

For phantom data, square regions of interest (ROIs) of uniform size (area, 2 cm^2) were carefully positioned in the center of the object on $\bar{D}$ and FA images obtained from both full-FOV single-shot EPI and SENSE EPI. The average values were estimated on every section. For human data, ROIs of variable size were positioned on the non–diffusion-weighted images by carefully avoiding contamination from CSF and, afterward, superimposed onto the calculated maps.

Discussion

Images were of a good quality for all the subjects studied. Figure 1 shows illustrative $\bar{D}$ and FA maps obtained from one subject. Although the SNR for any SENSE acquisition is bounded by an upper limit related to the geometry of the coils (which is not optimized in the standard neck coil that we used for this study), we have shown that SENSE DT MR imaging of the cord is feasible with a commercial machine, with no dedicated hardware, and it resulting in acceptable image quality.

A disadvantage of SENSE is the potential for residual aliasing artifacts on the unfolded images. Nevertheless, the geometry of the cord in the sagittal plane makes it particularly suitable for reducing the FOV in the phase-encoding direction, allowing for the choice of a simplistic approach for estimating

Values of $\bar{D}$, FA, and $\lambda_{/\!/}$ measured in cervical cord ROIs by using the SENSE EPI pulse sequence

Subject/Age, y/Sex	$\bar{D}$, $\times 10^{-3}$ mm^2/s	FA	$\lambda_{/\!/} \times 10^{-3}$ mm^2/s
1/29/F	1.18 (0.07)	0.50 (0.06)	1.95 (0.09)
1/29/F, repeat*	1.20 (0.06)	0.54 (0.05)	2.01 (0.15)
2/32/M	1.05 (0.02)	0.52 (0.07)	1.75 (0.07)
3/24/F	1.18 (0.08)	0.52 (0.06)	1.98 (0.16)
4/23/M	1.13 (0.05)	0.53 (0.07)	1.68 (0.10)
5/24/F	1.10 (0.05)	0.52 (0.05)	1.75 (0.08)

Note.—Data are the average (SD).

* Subject 1 was imaged again after a 7-day interval.

spatial sensitivity, with the advantage of being easily implemented and computationally efficient. Polynomial fitting gives enough smoothing to prevent aliasing due to small differences between the GE image and the SENSE acquisition. With the adopted $R = 2$, ghosts were virtually absent from the final images. Nonetheless, future work should focus on improving this estimate by using other methods (4), which present additional benefits.

In the phantom, the average $\bar{D}$ and FA obtained from the full-FOV EPI were 1.94×10^{-3} mm^2/s (SD, 0.002), and 0.001 (SD, 0.002), respectively; the average values obtained with the SENSE EPI were 1.89×10^{-3} mm^2/s (SD, 0.005) and 0.015 (SD, 0.001). These findings show that $\bar{D}$ assessment by means of SENSE is accurate, whereas FA measured by using SENSE EPI was higher than that measured with a standard full-FOV sequence. This result is not unexpected, considering the SNR limitations of SENSE and that FA estimation is particularly sensitive to noise (14, 15). Given the short acquisition time, an increase of the SNR could be achieved with more averaging. Comparing our in vivo results with previously published values is difficult because there is no general agreement about the normative diffusion data in the cord. Values of $\bar{D}$, FA, and the maximum eigenvalue ($\lambda_{//}$) for each subject are reported in the Table. The average values were $\bar{D} = 1.14\ (\pm 0.06) \times 10^{-3}$ mm^2/s, FA = 0.52 ($\pm$0.01), and $\lambda_{//} = 1.85\ (\pm 0.14) \times 10^{-3}$ mm^2/s. Because no criterion standard for cord segmentation exists, we chose to manually position the ROIs to avoid the inclusion of voxels not belonging to the cord. Given the small number of subjects studied, a single observer was able to perform this procedure in a reasonable time. The values of $\bar{D}$ that we measured in vivo are slightly higher than those seen in the previous literature, where they range from 0.9×10^{-3} to 1.2×10^{-3} mm^2/s (16–21), whereas the two studies performed by using DT MR imaging of the cord provided different estimates for FA and $\lambda_{//}$ (20, 21). We do not exclude the possibility that our results are partially influenced by CSF contamination, although we chose a relatively short TR to exploit T1 weighting and to provide around 15% attenuation of the signal intensity from CSF. If CSF contamination is present, it could be ameliorated either by increasing spatial resolution or by adding an inversion pulse to suppress CSF. However, both solutions would reduce the SNR

and increase the imaging time. Finally, images could be collected in the axial plane; however, an axial orientation would again require considerably longer acquisition times to cover the entire length of the cervical cord.

Conclusion

We have shown that SENSE combined with DT MR imaging can be implemented with a commercial system to assess water diffusivity characteristics of the cervical cord. Despite the reduction of SNR, we obtained good-quality images and off-resonance artifacts were reduced compared with those images acquired with a full-FOV EPI sequence. $\bar{D}$ and FA measured with this sequence were reproducible, although they were slightly different from those previously reported. Strategies to reduce potential CSF contamination are currently under investigation.

References

1. Pruessman KP, Weiger M, Scheidegger MB, Boesiger P. **SENSE: sensitivity encoding for fast MRI.** *Magn Reson Med* 1999;42:952–962
2. Basser PJ, Mattiello J, LeBihan D. **Estimation of the effective self-diffusion tensor from the NMR spin-echo.** *J Magn Reson B* 1994;103:247–254
3. Sodickson DK, Manning W. **Simultaneous acquisition of spatial harmonics (SMASH): fast imaging with radiofrequency coil arrays.** *Magn Reson Med* 1997;38:591–603
4. Bammer R, Keeling SL, Augustin M, et al. **Improved diffusion-weighted single-shot echo-planar imaging (EPI) in stroke using sensitivity encoding (SENSE).** *Magn Reson Med* 2001;46:548–554
5. Bammer R, Auer M, Keeling SL, et al. **Diffusion tensor imaging using single-shot SENSE-EPI.** *Magn Reson Med* 2002;48:128–136
6. Jones DK, Horsfield MA, Simmons A. **Optimal strategies for measuring diffusion in anisotropic systems by magnetic resonance imaging.** *Magn Reson Med* 1999;42:515–525
7. Tikhonov AN, Arsenin VY. **Solutions to ill-posed problems**. Washington: Winston; 1977
8. King KF, Angelos L. **SENSE image quality improvement using matrix regularization**. *Proceedings of the Ninth Scientific Meeting of the International Society of Magnetic Resonance Medicine.* Berkeley: International Society of Magnetic Resonance Medicine; 2001:1771
9. Ballester MAG, Machida Y, Kassai Y, Hamamura Y, Sugimoto H. **Robust estimation of coil sensitivities for RF subencoding acquisition techniques**. In: *Proceedings of the Ninth Scientific Meeting of the International Society of Magnetic Resonance Medicine.* Berkeley: International Society of Magnetic Resonance Medicine; 2001;799
10. Haselgrove JC, Moore JR. **Correction for distortion of echo-planar images used to calculate the apparent diffusion coefficient.** *Magn Reson Med* 1996;36:960–964
11. Jezzard P, Barnett AS, Pierpaoli C. **Characterization of and correction for eddy current artifacts in echo planar diffusion imaging.** *Magn Reson Med.* 1998;39:801–12
12. Studholme C, Hill DLG, Hawkes DJ. **Automated three-dimensional registration of magnetic registration of magnetic resonance and positron emission tomography brain images by multiresolution optimization of voxel similarity measures.** *Med Phys* 1997;24:25–35
13. Pierpaoli C, Basser PJ. **Towards a quantitative assessment of diffusion anisotropy.** *Magn Reson Med* 1996;36:893–906
14. Bastin ME, Armitage PA, Marshall I. **A theoretical study of the effect of experimental noise on the measurement of anisotropy in diffusion imaging.** *Magn Reson Imaging* 1998;16:773–785
15. Basser PJ, Pajevic S. **Statistical artifacts in diffusion tensor MRI (DT-MRI) caused by background noise.** *Magn Reson Med* 2000;44:41–50
16. Clark CA, Barker GJ, Tofts PS. **Magnetic resonance diffusion imaging of the human cervical spinal cord in vivo.** *Magn Reson Med* 1999;41:1269–1273
17. Clark CA, Werring DJ, Miller DH. **Diffusion imaging of the spinal cord in vivo: estimation of the principal diffusivities and application to multiple sclerosis.** *Magn Reson Med* 2000;43:133–138
18. Ries M, Jones RA, Dousset V, Moonen CTW. **Diffusion tensor MRI of the spinal cord.** *Magn Reson Med* 2000;44:884–892
19. Bammer R, Fazekas F, Augustin M, et al. **Diffusion-weighted MR imaging of the spinal cord.** *AJNR Am J Neuroradiol* 2000;21:587–591
20. Holder CA, Mukundan SJ, Eastwood JD, Hudgins PA. **Diffusion-weighted MR imaging of the normal human spinal cord in vivo.** *AJNR Am J Neuroradiol* 2000;21:1799–1806
21. Wheeler-Kingshott CAM, Hickman SJ, Parker GJM, et al. **Investigating cervical spinal cord structure using axial diffusion tensor imaging.** *Neuroimage* 2002;16:93–102